Effects of Mechanical and Chemical Properties on Transport in Fluoropolymers. II. Permeation

SANGWHA LEE[1] and KENT S. KNAEBEL[2]

[1] Department of Chemical Engineering, Kyungwon University, Seongnam City, Korea

[2] Adsorption Research Inc., 6185-D Shamrock Court, Dublin, Ohio 43016

Received 25 July 1996; accepted 16 August 1996

ABSTRACT: This is the second part of a study of chemical structure–physical property–performance relationships among several fluoropolymers and liquid penetrants, focusing on their permeation behavior. That behavior was consistent with the chemical and physical characteristics of the polymers, in that it depended on thermodynamic properties of the various penetrants (e.g., molecular volume, solubility parameters, and polarity). Relatively inert PFA showed effects only of molecular size. Similarly inert, but structurally modified ETFE showed nearly random dependence on all the properties. In contrast, ECTFE exhibited dipole–dipole bonds and PVDF embodied H-bonds; and both types of bonding affected permeability systematically. For example, ECTFE was most susceptible to polar compounds (dichloromethane and chlorobenzene), and PVDF was most susceptible to H-bonded liquids (phenol and methyl ethyl ketone).

The permeation behaviors of several combinations showed unusual dependence on time, thickness, and other factors such as temperature, processing conditions, chemical structure, and swelling due to relaxation. The Cattaneo–Maxwell model was used to fit transient permeation-rate data of relatively well-behaved ETFE. In contrast, a new kinetic model was devised to interpret more complex transient permeation behavior, particularly the observed acceleration in ECTFE. © 1997 John Wiley & Sons, Inc. J Appl Polym Sci **64:** 477–492, 1997

Key words: permeation; transport; mathematical models; fluoropolymers; properties

INTRODUCTION

Generalities

Fluoropolymers are paraffinic polymers that have some or all of the hydrogen replaced by fluorine. A fairly complete explanation of their nature is given in Part I of this paper. Rather than duplicate that material, the reader is referred there for background information. The purpose of this paper is to examine the effects of various chemical and mechanical properties on fluoropolymer permeability, so that they may be applied in practical situations.

Permeability

Compatibility of polymeric materials governs their suitability for nearly all potential applications. This is exploited through their ability to isolate fluids by serving as a barrier to mass transport. A quantitative measure of that ability is the permeability, which is equivalent to the product of solubility and diffusivity when both are spatially uniform. Permeability is an important factor in determining the suitability

Correspondence to: Kent S. Knaebel.

 CCC 0021-8995/97/030477-16

of a particular polymer for specific applications such as protective coatings, packaging materials, selective separations, biomedical devices, etc. Since permeation is governed by both the chemical and physical nature of the materials, understanding the underlying mechanisms of permeation can help in the selection of materials, as well as in product or process development. Furthermore, these phenomena are closely related to physical properties such as flexibility; free volume change; and structural and morphological features, such as the so-called "molecular probe" aspect.[1]

As explained in the next section, when both solubility and diffusivity are constant at any given temperature, the permeability is also a constant. In most cases involving organic liquids; however, these coefficients vary because of physical phenomena such as swelling, relaxation, deformation, and stress development in the matrix that occur simultaneously with the diffusion and solution process. Permeability may change from an initial value to a higher or lower value that is approached asymptotically; or the permeability may pass through an intermediate extreme, as was experimentally observed by Nguyen et al.[2] Such behavior is called non-Fickian, though the mechanisms and corresponding models that can represent such behavior vary widely (e.g., due to variations in diffusivity or solubility, or both).

This so-called non-Fickian behavior is an unfavorable phenomenon in the molecular design of advanced polymers for diverse applications including separation membranes, barrier polymers, and other high-performance applications. The penetrant absorbed by the polymer develops anisotropic swelling stress and promotes segmental motion of the polymer chains at any given temperature. In such cases, the permeability becomes a function of concentration, spatial coordinates, stress, and the history of a sample.[3]

Solubility Parameters

The fundamental question underlying the phenomena of solubility is about the nature and strength of intermolecular forces between solute and solvent. From a simplistic picture of intermolecular forces, a chemical will be a solvent for another material if the two molecules are compatible in the sense that the force of attraction between these molecules is not less than the forces of attraction between two like molecules of either species.

Hildebrand[4] used the latent internal energy of vaporization (ΔE_{vap}) to provide a useful measure of the attraction force holding molecules together. The theory is based on the concept of a "regular solution" with an ideal entropy of mixing and a nonideal enthalpy of mixing. The solubility parameter of a solvent, δ, was defined by the expression:

$$\delta = (\Delta E_{vap}/V_M)^{1/2} \quad (1)$$

where V_M is the molar volume of the solvent. This theory was initially developed for nonpolar substances having no specific interactions between the solute and solvent. Many solvents and polymers in common use, however, are polar and undergo specific interactions.

Later, Hansen[5] adopted the regular solution theory to polar substances by including a polar part divided into a dipole–dipole contribution (p) and a hydrogen-bonding contribution (h), which supplemented the dispersion (d) component. He named it a cohesion parameter.

$$\Delta E_{vap} = \Delta E_d + \Delta E_p + \Delta E_h \quad (2)$$

Combining the above equations gives:

$$\delta^2 = \delta_d^2 + \delta_p^2 + \delta_h^2 \quad (3)$$

Solubility parameters never completely describe the interactions between polymers and solvents. Only the enthalpy term (ΔH) is considered in the solubility parameter theory, even though the entropy of mixing (ΔS) should be considered to describe the miscibility. Despite that, solubility-parameter approaches can be good guides and have been used widely.

Just as permeability depends on the solubility and diffusivity, polymer swelling depends on the solubility of the solvent in the polymer. The degree of swelling of the polymer is a maximum when the solubility parameters match. The values of Hildebrand solubility parameters for specific polymers thus may be determined experimentally by observation of degrees of swelling in a spectrum of solvents with known Hildebrand parameters. In addition, the electronic and chemical structure of the polymer can be elucidated experimentally through the choice of solvents with known solubility parameters, cohesion parameters, and hydrogen-bonding capability. This approach is discussed later in the context of selection

of solvents and in the context of interpretation of experimental results.

Objectives and Scope

The main goal of this paper is to explain some of the chemical structure–physical property–performance relations among polymers and organic chemicals. It may provide a step towards obtaining a systematic and comprehensive view of transport properties of fluoropolymers, and it may provide information about the molecular nature of the polymer chains. This objective is pursued by relating the polymer and penetrant properties to the performance of polymeric materials via mathematical models which are discussed later.

This work focuses on measurements of permeability of some organic liquids in several fluoropolymers in order to evaluate the systematic relationships between polymer structures and transport properties. The scope is currently limited to studies of PFA, ETFE, ECTFE, PVDF, and FEP. The penetrants are benzene, toluene, and chlorobenzene. Others, such as phenol, methyl ethyl ketone and dichloromethane, are included in some tests to explore some specific effects. Other aspects considered are polymer thickness, temperature, orientation, and repeated exposures. Finally, a kinetic model is developed to better understand the complex observations of permeation rates for certain systems.

THEORY

Solution-Diffusion Theory

The transport of a penetrant, A, through a homogeneous membrane, in the absence of gross defects such as pores or cracks, is usually considered to occur by the following process: (1) solution of the gas or vapor in the surface layers, (2) migration to the opposite surface under a concentration (chemical potential) gradient, and (3) devolution from that surface into the ambient phase. Such a view of the diffusion of gases through solids was first proposed in 1866 by Graham.[6] If the evaporation process is not the rate-determining step, the constant of proportionality in the rate equation, which is called permeability (P_A) can be expressed as the product of solubility (S_A) and effective diffusivity (D_A), if there is a linear relationship between concentration, (C) and pressure (p).

$$J_A = D_A \frac{(C_{A_1} - C_{A_2})}{l} = D_A \cdot S_A \frac{(p_{A_1} - p_{A_2})}{l} \quad (4)$$

where $P_A = D_A \cdot S_A$. For liquids, ignoring osmotic pressure, solubility in a polymer is defined differently from gases. Conversely, effective diffusivity has practically the same definition, viz., $P_A = D_A \cdot K_A$, where $K_A = \bar{C}_A$ (solid phase)/C_A (liquid phase). In the following paragraphs, the subscript A will be omitted for convenience.

Solubility is a thermodynamic property and diffusivity is a kinetic property. Rubbers commonly exhibit ideal behavior, and the diffusion coefficient frequently varies with temperature by an Arrhenius relationship[7,8]:

$$D = D_0 \exp(-E_D/RT) \quad (5)$$

where D_0 is the pre-exponential factor, E_D is the activation energy for diffusion, R is the gas constant, and T is the absolute temperature. Likewise, the solubility coefficient, S, varies with temperature, approximately according to the van't Hoff relationship:

$$S = S_0 \exp(-\Delta H_s/RT) \quad (6)$$

where S_0 is the pre-exponential factor, and ΔH_s is the enthalpy change upon dissolution of the liquid in the polymer. Idealized behavior results not only from Fickian diffusion, but also from Henry's law of solubility. Combining these, the temperature dependence of permeability can be represented by:

$$\ln\left(\frac{P(T_2)}{P(T_1)}\right) = \ln\left(\frac{D(T_2)\cdot S(T_2)}{D(T_1)\cdot S(T_1)}\right) = -\frac{\Delta H_s + E_D}{R}\left(\frac{1}{T_2} - \frac{1}{T_1}\right) \quad (7)$$

The absolute value of ΔH_s (usually positive) is usually larger than that of E_D (usually negative), so permeability normally increases with temperature.

There is, however, considerable evidence which suggests that this simple model is not adequate for viscoelastic materials such as glassy polymers and semicrystalline polymers at high activities of organic vapors or liquids. The major shortcoming of this simple theory is that it cannot treat the very complex time-dependence of diffusivity and

solubility that results when mass transport is coupled with structural relaxation of polymeric materials associated with a glass transition.

Cattaneo–Maxwell Theory

No comprehensive model for diffusion in polymers is available. Such a model for diffusion would require consideration of structural deformation, stress fields, and possibly heat transfer.[9] A model that incorporates some of these features is based on a viscoelastic constitutive equation that accounts for the diffusive mass flux in order to predict some non-Fickian effects that were observed in certain polymer–penetrant systems. A specific example is the Cattaneo–Maxwell (C–M) model which is actually a truncated form of a more general relation originally derived by Maxwell from kinetic considerations.[10] It was simplified by neglecting the velocity of the center of mass; in that case, the C–M equation took the form[11]:

$$J + \tau \frac{\partial J}{\partial t} = -D\nabla\nu \qquad (8)$$

where J and ν are the diffusive volume flux and the volume fraction of penetrant species, while D and τ may be functions of concentration.

Equation (8) was first used to simulate non-Fickian diffusion by Camera-Roda and Sarti.[11] In their model the diffusivity, D, and the relaxation time, τ, were assumed to vary with the concentration according to the free-volume theory. Their numerical solution considered first-order relaxation of surface concentration, and it represented well both Case II and anomalous diffusion, as well as the frequently observed overshoot and oscillations in the weight uptake around the final equilibrium value. Later, the C–M equation was considered as a relaxational diffusive flux term to be added to the classical Fickian expression.[12,13]

In the simplified C–M model, τ represents a relaxation time or build-up period for the commencement of mass flow after a concentration gradient has been imposed on the medium. That is, mass flow does not start instantaneously but increases gradually with a relaxation time, τ, after the application of a concentration gradient. Similarly, the mass flow does not cease immediately, but diminishes gradually after the concentration gradient is removed.[14] Once steady-state is achieved, the C–M equation reduces to Fick's law with D as the diffusion coefficient. Also, the situation $\tau \to 0$ leads to diffusion with an instantaneous relaxation, which also coincides with Fick's law.

To solve the C–M equation analytically for transient permeation, τ and D are assumed to remain constant over the relevant concentration range, and the last term of eq. (8) is also approximated by Fick's transient flux equation which is discussed in the next section. If only the first term of the Fickian transient flux equation is used, an analytical solution can be found by employing an exponential integrating factor and initial condition:

$$\bar{J} = J/J_s = -e^{-t/\tau} \int_0^t e^{t'/\tau}[1 - 2\exp(-\pi^2 Dt'/l^2)]dt' \qquad (9)$$

subject to the initial condition: $J = 0$, $t = 0$, $x = l$, where J_s is a steady-state diffusive flux and l is a thickness of the membrane. The resulting analytical equation is:

$$\bar{J} = 1 - e^{-t/\tau} - 2\frac{[\exp(-\pi^2 Dt/l^2)] - e^{-t/\tau}}{1 - \pi^2 D\tau/l^2} \qquad (10)$$

where D may represent a relaxational diffusivity, not simply the constant diffusion coefficient. This analytical equation reduces to the simple Fickian diffusive flux equation as $\tau \to 0$. In addition, the normalized diffusion flux approaches to unity as $t \to \infty$.

If the variation of τ is large enough to exhibit apparent relaxation effects, the above analytical solution may not be valid. Better insight into the polymer–penetrant system during transient permeation, however, could then be obtained by allowing variation of the relaxation time in the transient regime. The simplest, reasonable time dependence of τ is:

$$\tau = \tau_0 \exp(-kt) \qquad (11)$$

This expression follows from a first-order response of the polymer to the penetrant, in going from its initial condition to steady state. The values of τ_0 and k may depend on the polymer and penetrant, as well as temperature, thickness, and prior exposure.

Kinetic Theory

As previously shown in the kinetic model for the transient sorption, nonlinear characteristics of

transient permeation may also be described by structural changes, which may be simply expressed by the creation of free volume in the polymer matrix. In many, if not most experiments, the polymer is initially free of the penetrant; and the concentration at the downstream face is nil. For Fickian diffusion, the total amount of diffusing substance, Q, which has passed through the membrane in time t, is given by[15]:

$$\frac{Q}{lC_1} = \frac{D_F t}{l^2} - \frac{1}{6} - \frac{2}{\pi^2}\sum_1^\infty \frac{(-1)^n}{n^2}\exp(-\pi^2 n^2 D_F t/l^2) \quad (12)$$

where D_F is a constant Fickian diffusivity. The flux equation, thus, can be obtained by the differentiation of eq. (12), and is given by:

$$\bar{J}_F = 1 + 2\sum_1^\infty \frac{(-1)^n}{n^2}\exp(-\pi^2 n^2 D_F t/l^2) \quad (13)$$

Transient permeation coupled with structural deformation, however, cannot be simply expressed by the Fickian mechanism because the solubility, diffusivity, and concentration gradient all change, depending on the concentration of the penetrant and the history of the sample, as well as the swelling stress. As suggested by Berens and Hopfenberg,[16] the transient flux at any time, t, may be split into two portions:

$$\bar{J} = (1 - \alpha)\bar{J}_F + \alpha\bar{J}_R \quad (14)$$

where $1 - \alpha$ represents the fraction of Fickian diffusive flux, J_F, driven by the concentration gradient developed in the original free volume, and α represents the fraction of relaxational diffusive flux, J_R, driven by the concentration gradient developed in the created free volume.

Returning to the equation for the transient flux and considering the outer thin layer downstream, the transient flux at $x = l$ could be expressed approximately as follows:

$$J|_l = -D\left.\frac{\partial c}{\partial x}\right|_l = -\frac{D}{\Delta\epsilon}[C(l, t) - C(l - \Delta\epsilon, t)] \quad (15)$$

where $C(l, t)$ is usually negligible in most practical situations. For a very small value of $\Delta\epsilon$, the flux equation at the utmost surface can be simply expressed as a linear combination of concentration and diffusivity in time t during the transient period.

The net fractional increase of concentration due to relaxation is $(C_f - C_{f0})/(C_{f\infty} - C_{f0})$ in the context of local concentration, where the concentration of penetrant in the new (or created) free volume at a specific time is C_f; and that of penetrant in the original free volume is C_{f0} and, at equilibrium, $C_{f\infty}$. The free-volume fraction, f, is assumed to be linearly related to the concentration as $C_f = k_1 + k_2 f$, where k_1 and k_2 are constants according to eq. (4) in Lee and Knaebel.[17]

The permeability can be expressed as the same type of transient flux equation, assuming linear dependence of solubility on the volume fraction of the penetrant, ν[18]:

$$\begin{aligned} S &= S_0 \exp(\gamma_s \nu) \\ &= S_0(1 + \gamma_s \nu) \\ &= S_0[1 - (\gamma_s/\gamma_f)f_0 + (\gamma_s/\gamma_f)f] \\ &= k_3 + k_4 f \end{aligned} \quad (16)$$

where, $\gamma_s \ll 1.0$, $f = f_0 + \gamma_f \nu$.

Based on the similar dependence of relaxational flux and permeability on free volume, it is assumed that a function involving the difference between P and P_0 is proportional to the instantaneous relaxational flux during transient permeation and that a similar function of P and P_∞ is proportional to the difference of the ultimate flux and that which would occur through the unrelaxed membrane. Therefore, the limiting indications of no change and ultimate change during transient permeation are P_0 and P_∞, respectively. The transient permeability falls somewhere between these two limiting values. Applying the inverse lever principle to this function, the fractional flux due to relaxation, F_R, is taken as[19]:

$$F_R = \bar{J}_R = \frac{J - J_F}{J_\infty - J_F} = \frac{g(P) - g(P_0)}{g(P_\infty) - g(P_0)} = \frac{P - P_0}{P_\infty - P_0} \quad (17)$$

where $g(P) = B \cdot P$. The function, $g(P)$, relates the degree of the structural change to the permeability, and B is a constant. When the permeabil-

ity is constant, no relaxational flux occurs, e.g., there is no structural deformation or buildup. Likewise, as the permeability approaches a value of P_∞, there is no further change in polymer structure.

Power Dependence of the Rate Equation

It is assumed that the flux due to structural change is proportional to $1 - F_R$, the unrelaxed fraction, via a pseudofirst order mechanism as in the transient sorption case:

$$1 - F_R \overset{k_f}{\rightharpoonup} F_R \tag{18}$$

$$\frac{dF_R}{dt} = k_f(1 - F_R) \tag{19}$$

The rate coefficient, k_f, may depend on penetrant concentration because higher concentration of penetrant produces a faster rate of structural change. A simple exponential function is proposed to relate the permeability and rate constant to the penetrant volume fraction.[18]

$$P = P_0\exp[(\gamma_s + \gamma_D)\nu] \tag{20}$$

$$k_f = k_{f0}\exp(\gamma_k\nu) \tag{21}$$

When the above expressions are combined, the rate coefficient can be expressed as a power function of permeability.

$$k_f = k_{f0}\exp\left[\left(\frac{\gamma_k}{\gamma_s + \gamma_D}\right)\ln(P/P_0)\right] \tag{22}$$

$$k_f = k_{f0}(P/P_0)^K \tag{23}$$

The resulting rate equation is:

$$\frac{dF_R}{dt} = k_{f0}[1 + (\theta - 1)F_R]^K(1 - F_R) \tag{24}$$

where $\theta = P_\infty/P_0$.

This permeation rate model [eqs. (13), (14), and (24)], has five adjustable parameters: (1) α = fraction of total transient flux due to relaxation effects; (2) D_F (cm^2/day) = Fickian diffusivity or intrinsic diffusivity; (3) k_{f0} (1/day) = rate coefficient; (4) θ = permeability ratio, P_∞/P_0; and (5) K = ratio of sensitivity coefficients, $\gamma_k/(\gamma_s + \gamma_D)$.

If $K = 1$, the rate equation can be solved analytically, as was the quadratic rate equation for transient sorption. If $K \neq 1$, the resulting equation must be solved numerically.

EXPERIMENTS

The purpose of the experiments described below was to measure permeability of several substances in a variety of polymers, over a range of temperatures and polymer thicknesses. The results provide a basis for predicting the barrier properties of the polymers. They also reveal subtle effects of processing conditions (e.g., roll coating orientation and formulation) that may be useful for product development. The experiments often yielded unusual behavior, which was subsequently explained in the context of model parameters.

Organic Solvent Selections

The penetrants selected for these experiments generally can be classified as two types, based on their molecular structures: aromatics and other organics. The penetrants also can be broadly categorized by their chemical properties: nonpolar, polar, and H-bonding. For instance, benzene and toluene are nonpolar. Chlorinated-organics, such as chlorobenzene and dichloromethane, are usually polar. Phenol and methyl ethyl ketone (MEK) are considered to be H-bonding, which is usually stronger than dipole–dipole interactions.

All the organic chemicals were liquids at ambient conditions (25°C, 1 atm). A list of liquids and their properties, including Hansen solubility parameters with three subdivisions: dispersion (δ_d), hydrogen-bonding ability (δ_h), and polar contribution (δ_p), and including electrostatic properties [such as dipole moment (μ) and polarity (P)], is given in Table I. Gordon[20] discussed the nature of molecular interactions in terms of the fraction of total interaction due to dipole–dipole (p), induction (i), and dispersion (d) effects such that $p + i + d = 1$.

Experimental Methods, Apparatus, and Conditions

In our experiments, the permeation rate was determined by measuring the rate of mass loss of a penetrant through a polymer film to air from an otherwise closed vessel (as described below). Thus, permeation was observed under quasi-steady state conditions. As a result, the permeation data could be analyzed as a boundary value

Table I Solubility Parameters and Related Properties

Solvent	V_m	δ	δ_d	δ_p	δ_h	H-bonding	P	μ
C_6H_6	89	18.6	18.4	0.0	2.0	poor	0.000	0.0
$C_6H_5CH_3$	107	18.2	18.0	1.4	2.0	poor	0.001	0.4
C_6H_5Cl	102	19.6	19.0	4.3	2.0	poor	0.058	1.6
C_6H_5OH	89	24.1	18.0	5.9	14.9	moderate	0.057	1.6
CH_2Cl_2	65	20.3	18.2	6.3	6.1	poor	0.120	1.8
$CH_3COC_2H_5$	90.1	19.3	14.1	9.3	9.5	moderate	0.510	3.3

Units: V_m (cm^3/mol), δ ($MPa^{1/2}$), μ (Debye), P (dimensionless).

problem. The mass transfer resistances from the bulk penetrant to the polymer surface and from its outside surface into ambient air were assumed to be insignificant. Therefore, the permeability was determined directly from the measurement of the mass flux.

Each test of a liquid permeating through a polymer sample into air closely followed the current ASTM method for evaluating vapor transmission of volatile liquids. The permeation experiments were conducted in cup-shaped vessels made of 316 stainless steel and Carpenter 20, as shown schematically in Figure 1. The permeation cells were 5.08 cm deep and 6.35 cm inside diameter. Eight allen screws held the flange together.

Approximately 50 ml of an organic liquid was added to each vessel; and the polymer disk was placed onto the cup opening, followed by an annular VITON gasket and capped by the top flange. The allen screws were tightened evenly and securely. After that, the permeation chambers were inverted so that the liquid inside was in direct contact with the polymer disk, penetrating downward. The permeation vessels were kept in a fume hood at room temperature or in a ventilated convection oven at high temperature. The mass of the permeation chambers was usually measured every four days using a Mettler PM1200 balance having an accuracy of ±1.0 mg.

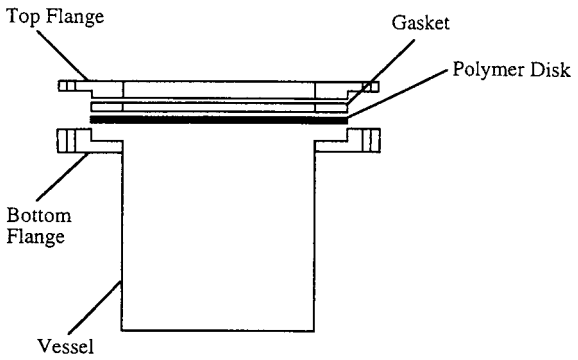

Figure 1 Apparatus for measuring liquid permeation rates.

Blank experiments, in which the permeation vessels contained polymer disks but no liquids, were conducted to compensate for extraneous effects such as humidity and dust. Fluctuations of the mass of the empty chambers were taken into account by subtracting the mass gain of blank vessels from the total mass of the filled vessels.

Variables that were systematically tested included: the thickness of the sample (0.25 and 2.3 mm), temperature (25°, 45°, and 75°C), and the liquid penetrants (benzene, toluene, chlorobenzene, MEK, dichloromethane, and phenol). Several fluoropolymers were tested: ETFE, ECTFE, PVDF, PFA, and FEP.

Data Analysis

The experimental data were analyzed and tabulated using a commercial spreadsheet program. The permeation rate at steady state was calculated via the linear regression option. Only steady-state permeation data were used in the calculation, excluding the initial transient period. The rate of permeation was reported in units of (g/m^2/day). To ensure statistical validity, at least three replicates of each experiment were completed. When the three average permeation rates were within a reasonable standard deviation of their mean, the mean was calculated and reported as the permeation rate at those sets of conditions.

EXPERIMENTAL RESULTS AND DISCUSSION

Application of Model Equations to Experimental Rate Data

In transient sorption, ETFE film exhibited a slightly distorted Fickian sorption curve with a

slight inflection point near the outset of sorption, and ECTFE film produced a non-Fickian sorption curve which showed an accelerating uptake as equilibrium was approached. Similarly, during transient permeation, ETFE exhibited seemingly Fickian behavior, and ECTFE exhibited distinct non-Fickian behavior. In particular, the initial permeation rate in ECTFE film was very low, but increased rapidly as time proceeded due to relaxation effects. These two behaviors were analyzed by the Cattaneo–Maxwell model and the new kinetic model, respectively. For ECTFE, the fitted parameters from the C–M model varied drastically, e.g., relaxation times from $\sim 10^5$ days to ~ 1 day during the transient period of permeation. On the other hand, much less variation of relaxation time (e.g., $10^2 \sim 1$ days) was observed in ETFE (0.254 mm)-benzene at 45°C.

The power type of rate equation was again applied to fit the anomalous permeation rate data for ECTFE-aromatic solvents which exhibited a sudden jump from a low permeation rate (due to Fickian diffusion) to a high permeation rate (due to relaxation effects). The permeation rate data were taken as an average value for each quasi-steady-state region because the data points were too scattered to obtain a best fit. In some cases, the initial permeation rate data were too scattered to get meaningful values of the Fickian diffusivity, D_F. Therefore, fitted values were used to represent the relative trends of relaxational behavior during transition observed in ECTFE-penetrant systems at 25°C.

The relaxation fraction, α, was determined from experimental data as the ratio of low permeation rate to high permeation rate, which reduced the number of adjustable parameters from 5 to 4. As shown in Table II, the ratio of sensitivity coefficients, K, ranged from 1.5 to 1.7, which was higher than the ratio, $\gamma_k/\gamma_D (\sim 1)$, from the transient sorption model. This implies that relaxation affects flux more than transient sorption. The Fickian diffusivity, D_F, turned out to be nearly constant, irrespective of the solvent type.

In contrast, the fitted value, k_{f0}, revealed the impact of nonisotropic structure on permeation. For example, the ECTFE exhibited a shiny side and a dull side, due to processing conditions. In that vein, permeation rates measured from the dull side toward the shiny side were higher than those in the reverse direction. This indicates that the relaxational flux for the latter is faster than for the former, which will be described in detail.

In addition, the lower permeability ratio, θ, obtained for the shiny side indicated that the solubility and probably the diffusivity of the surface skin (in the shiny side) was lower than that of the soft skin (the dull side), at equilibrium. Specifically, the permeability ratio was the same order of magnitude as the diffusivity ratio (e.g., $100 \sim 200$), as obtained from our corresponding sorption rate model in the companion paper,[17] although the permeability ratio was smaller than the diffusivity ratio. This inconsistency may have been caused by the linear approximation between permeability and relaxational flux (which is admittedly a rough approximation) or may have been due to inaccurate parameter estimation because of scatter.

Table II Fitted Rate Parameters of Aromatic Solvents in ECTFE (0.25 mm)-Benzene at 25°C

Penetrants	Parameters	Dull Side	Shiny Side
Benzene	α	0.85	0.93
	$D_F \times 10^4$	1.10	1.02
	$k_{f0} \times 10^4$	5.48	3.84
	θ	110	76.7
	K	1.5	1.7
Toluene	α	0.88	0.89
	$D_F \times 10^4$	1.09	1.01
	$k_{f0} \times 10^4$	4.12	3.63
	θ	82.4	72.5
	K	1.6	1.6
Chlorobenzene	α	0.91	0.99
	$D_F \times 10^4$	1.04	0.81
	$k_{f0} \times 10^4$	4.69	4.03
	θ	93.7	80.7
	K	1.7	1.6

If not specified, the thickness of polymer samples will be considered to be 0.25 mm.

Experimental transient permeation rates are compared with estimates of the C–M model [eq. (10)] and the power-type of kinetic model [eqs. (13), (14), and (24)] in Figure 2 for ETFE-benzene at 45°C and ECTFE-benzene at 25°C, respectively. The values of the fitted parameters are listed in Table II. They appear to represent the observed transient permeation curves in a consistent manner, though it is premature to claim that physical understanding can be drawn from this model.

Polymer and Solvent Types

For a homologous series of aromatic solvents, fluoropolymers (PFA, ETFE, and PVDF) showed

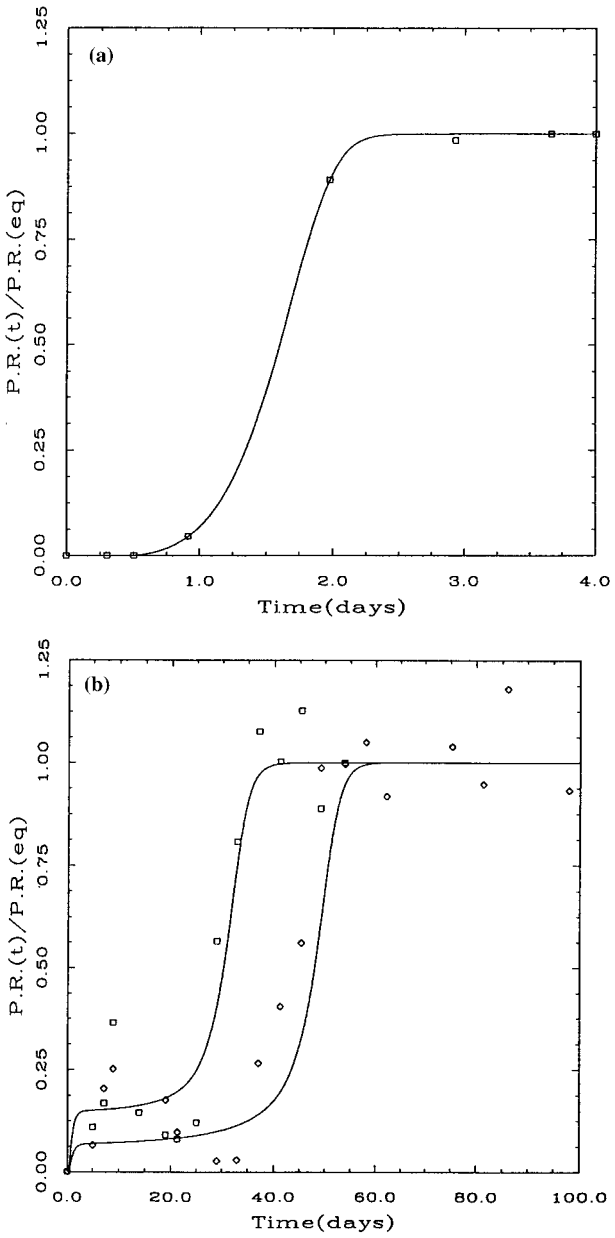

Figure 2 Fitted permeation curves by the analytical C–M model (a) and the power type of kinetic model (b) (□: Dull side; ◇: Shiny side). If not specified in the following figures, the thickness of polymer samples will be considered 0.25 mm.

the same trends of permeation behavior according to the degree of their geometric and electronic characteristics, respectively. Small and nonpolar benzene produced the highest permeation rate among aromatic solvents. If a penetrant is not very polar, its size becomes a critical factor in determining its permeation rate. For example, nonpolar toluene and polar chlorobenzene exhibited almost the same permeation rate due to their similar sizes. In ECTFE, however, polar chlorobenzene gave a higher permeation rate than nonpolar toluene, due to polar–polar interactions, as shown in Figure 3(a), (b), and (c) (see Table V).

Perfluorinated films (FEP and PFA) always showed excellent barrier properties, e.g., low permeation rates for organic chemicals, compared with the other fluoropolymers. Their behavior was very similar, as expected from the fact that their chemical and physical structures are also almost identical. Contrary to the expectation for the performance of perfluorinated resins, modified fluoropolymers (ETFE, ECTFE, and PVDF) showed different permeation behaviors for different types of solvents. For example, ECTFE turned out to be most suscep-

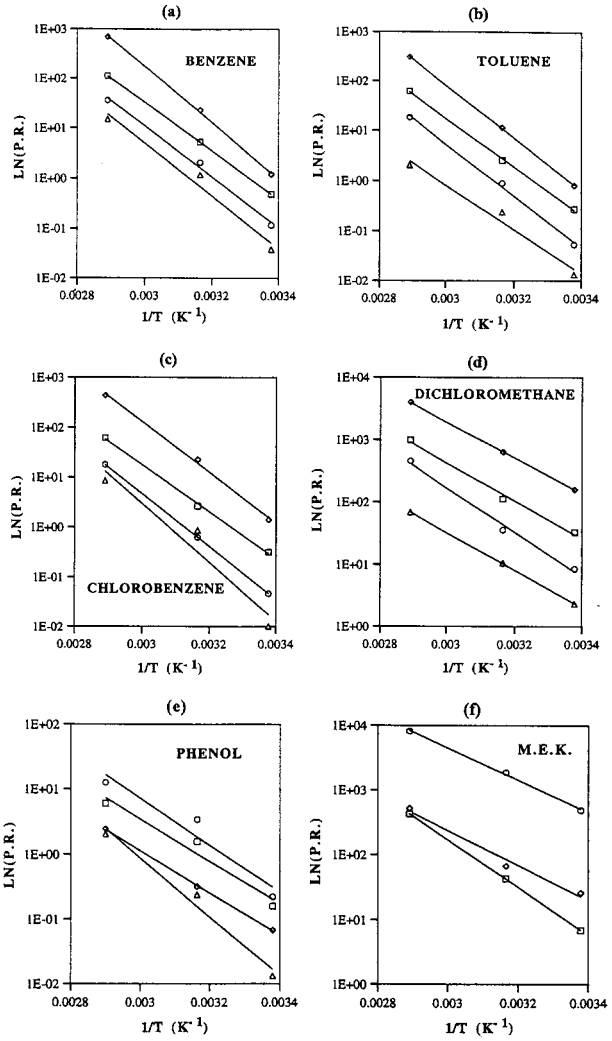

Figure 3 Arrhenius plots of permeation rates of various organic liquids in fluoropolymers (□: ETFE, ◇: ECTFE, ○: PVDF, △: PFA).

Table III Susceptibility of Fluoropolymers to Various Types of Solvents

	Permeation Rates	
	High	Low
Nonpolar (C_6H_6, $C_6H_5CH_3$)	ECTFE-ETFE-PVDF-FEP/PFA	
Polar (C_6H_5Cl, CH_2Cl_2)	ECTFE-ETFE-PVDF-FEP/PFA	
H-bonding (C_6H_5OH, $CH_3COC_2H_5$)	PVDF-ETFE-ECTFE-FEP/PFA	

tible to polar chlorinated hydrocarbons, as shown in Figures 3(c) and (d). On the other hand, PVDF was most susceptible to H-bonding organics such as phenol and methyl ethyl ketone, as shown in Figures 3(e) and (f). ETFE exhibited intermediate resistance to polar and H-bonding organics among the modified fluoropolymers, as shown in Figures 3(a)–(f). The trends of permeation behavior are summarized in Table III.

It is generally accepted that modified fluoropolymers are highly resistant to penetration of small gas molecules due to the increased strength of their polar intersegmental interactions. In liquid permeation cases, however, modified fluoropolymers gave higher permeation rates than perfluorinated films due to the disruption of polar intersegmental bonds. As mentioned earlier, the character of the interchain bonds in PVDF is more protonic, and the bonds in ECTFE have the character of dipole–dipole interactions. ETFE has both characteristics, but the strength of interchain bonds is less protonic in character than in PVDF and less than that in ECTFE in dipole–dipole interactions.

Effects of Processing Properties

Surface Skin

ECTFE films also exhibited other unusual behaviors due to the existence of a dense shiny skin that was possibly formed during manufacturing using a take-up roll when the surface exposed to air became soft and dull. The two different surfaces apparently had different properties. The shiny skin seemed to be more tough and resistant to swelling stress than the dull side. This was illustrated by the onset of rapid relaxation of different time scales, depending on the type of penetrating solvent and the types of exposed surfaces.

Small and polar penetrants such as benzene and chlorobenzene induced faster relaxation in ECTFE film, resulting in a rapid increase of the permeation rate during the transient period, compared with the larger toluene, as shown in Figure 4. Exposing the tough skin to the penetrant led to slower relaxation in comparison to exposing the dull side, as shown in Figure 5. In addition, the onset of rapid relaxation, especially when the shiny side was exposed to the penetrant, appeared

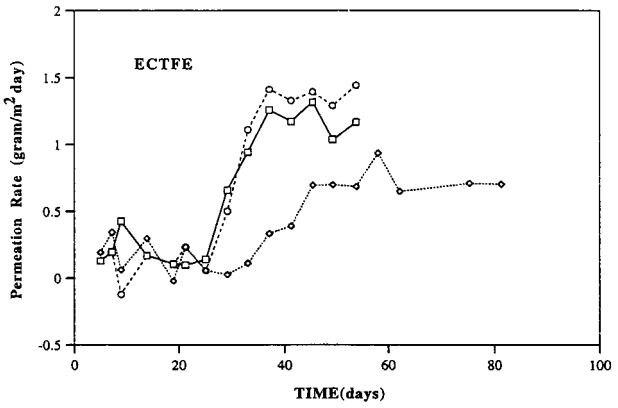

Figure 4 The transient permeation rate of aromatic solvents through ECTFE at 25°C (□: Benzene, ◇: Toluene, ○: Chlorobenzene).

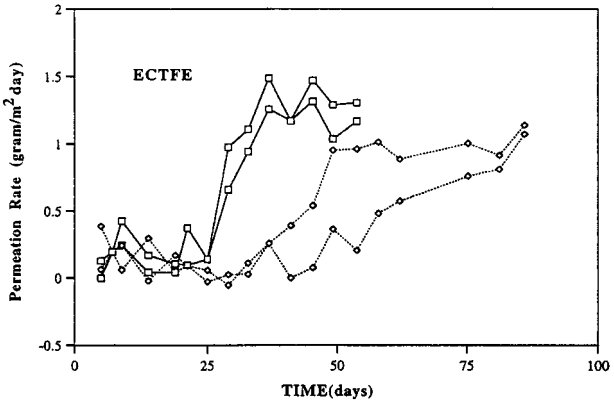

Figure 5 The comparison of permeation rates of benzene in ECTFE, when the shiny side is exposed, and when the dull side is exposed at 25°C (□: Dull side, ◇: Shiny side).

Table IV Comparison of Permeation Rate and Steady-State Uptake for Thin ECTFE Samples Exposed to Permeant on the Dull (Soft) Side or Shiny (Tough) Side

Properties	Temp. (°C)	Benzene		Toluene		Chlorobenzene	
		D[a]	S[a]	D[a]	S[a]	D[a]	S[a]
Permeation rate ($g/m^2/day$)	25	1.190 8	1.050 6	0.789 7	0.690 7	1.406 1	1.283 3
	45	22.37 6	17.22 1	11.36 8	9.546 9	22.50 3	19.50 2
Sorbed mass[b] (g/g)	25	0.052 1	0.047 2	0.044 0	0.042 9	0.063 5	0.055 9
	45	0.059 4	0.053 1	0.049 9	0.045 9	0.067 2	0.059 8

[a] D: Dull side, S: Shiny side.
[b] Sorbed Mass: The mass change of each polymer disk used in permeation experiments.

with different time scales, e.g., the distribution of relaxation times, which are generally observed in glass transition phenomena.

The steady-state permeation rate when the shiny side was in contact with the solvent was slightly less than that of the dull side, as shown in Table IV. This indicates that the shiny side is less permeable and probably exhibits lower solubility than the dull side. Conversely, the diffusivity difference alone could not account for the observation, any more than the overall resistance of a series of resistors depends on the sequence of individual resistors.

Overshoot

Overshoot was exhibited during some permeation experiments with ECTFE as shown in Figure 6. This anomalous behavior was not detected clearly at room temperature, but at 45° and 75°C it was clearly observed. After the permeation rate reached its maximum, it leveled off and dropped to a lower, steady value. This phenomenon implies that the relaxation process, during transient permeation, creates a supersaturated space which can accommodate penetrants into the polymer matrix, but which is not thermodynamically stable (possibly in microvoids that are subsequently "healed"). The overshoot of the permeation rate cannot be explained by the mechanism of Case II sorption. It may originate from a combination of structural factors due to chemical composition and processing conditions.

Thickness Effects

The effect of thickness on permeation rate is shown in Figure 7. As can be seen, the permeation data were reanalyzed by considering thickness explicitly in terms of permeability, i.e., the product of permeation rate ($gram/m^2day$) and sample thickness (mm).

At 45°C, ECTFE samples exhibited roughly the same permeabilities for both thin and thick films. The thick films (2.3 mm) of the other polymers, ETFE and PVDF, oddly exhibited much higher permeation rates than the thin films (0.25 mm). At 75°C, however, thin films exhibited much higher permeabilities than thick films of ECTFE and ETFE. The weak sensitivity of thick films to temperature may be responsible for this result; thin films exhibited much higher sensitivity to temperature change. These materials were obviously not isotropic since the permeation rates were not inversely related to thickness.

According to permeation theory for isotropic materials, following Fick's law, the permeation rate should be inversely proportional to the thickness of the polymer sample. In a practical sense, however, thickness dependence anomalies occur because of polymer processing conditions and resulting nonisotropy.[21] That is, physical properties may vary with depth in the polymer even though the polymer has a homogeneous chemical structure, e.g., the skin at one or both surfaces may be more dense and impermeable than the core. Our findings unfortunately did not discern the precise cause of the unusual thickness effects.

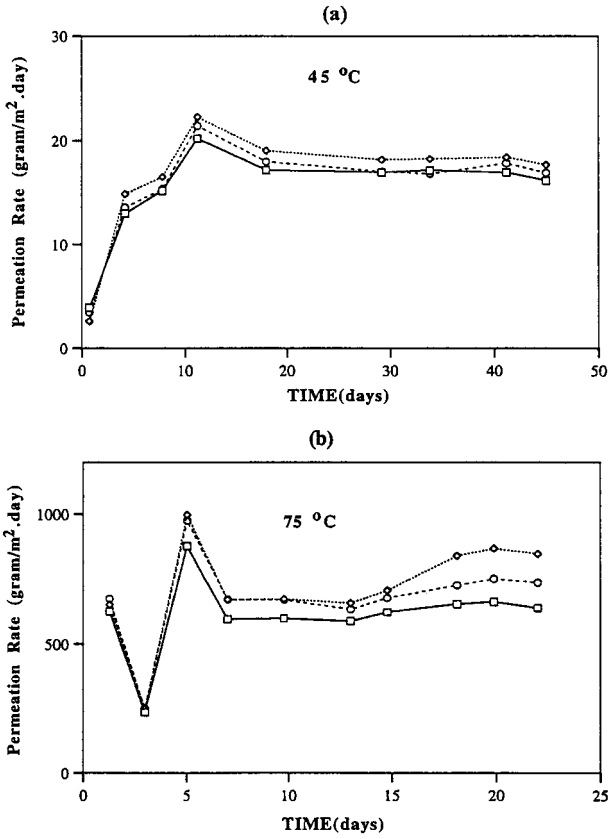

Figure 6 Overshoot in transient permeation of ECTFE-benzene system at 45° and 75°C (□: Sample 1, △: Sample 2, ○: Sample 3).

Temperature Effects

Permeation rates were measured at each of three successive temperatures (25°, 45°, and 75°C) for various types of penetrants. In Table V, the permeation rates only of homologous aromatic liquids are shown for the three different temperatures. The permeation behavior of all three polymers (0.254 mm thick) was highly sensitive to temperature: each exhibited increases of factors of 200 to 300 in permeation rate over the 50°C span. Apparent activation energies of permeation were obtained using eq. (7) and are shown in Table VI and Figure 8.

The activation energies for ETFE and PVDF of aromatic solvents depend mostly on size rather than polarity or electronic factors, in that the activation energy is about the same for both toluene and chlorobenzene, but it is twice as large for benzene. Conversely, in ECTFE the activation energies between toluene and chlorobenzene are different, indicating that the barrier properties of ECTFE are different than those of PVDF and ETFE. It is still the largest for benzene and is smaller by a factor of two for toluene. Chlorobenzene is intermediate, probably indicating not only a size effect but also a polarity effect, as alluded to previously.

The temperature dependence of permeation rate of PFA deviated somewhat from eq. (7), as shown in Figure 9. This may result from crossing a glass transition temperature within the temperature range. Additional evidence was that the sorption curve at 45°C exhibited more distinct deviation from Fickian sorption curve compared with those at 25° and 65°C, as shown in the companion paper (in Figure 7 of Part I. Sorption)[17]. PTFE is known to have a glass transition around 30°C,[22] and PFA is very similar to PTFE in terms of chemical and physical properties. More evidence, e.g., DSC data, is required to reach firm conclusions.

Effects of Thermodynamic Properties on Transport Properties

It is intuitive to expect that permeation rates correlate with general physical parameters such as

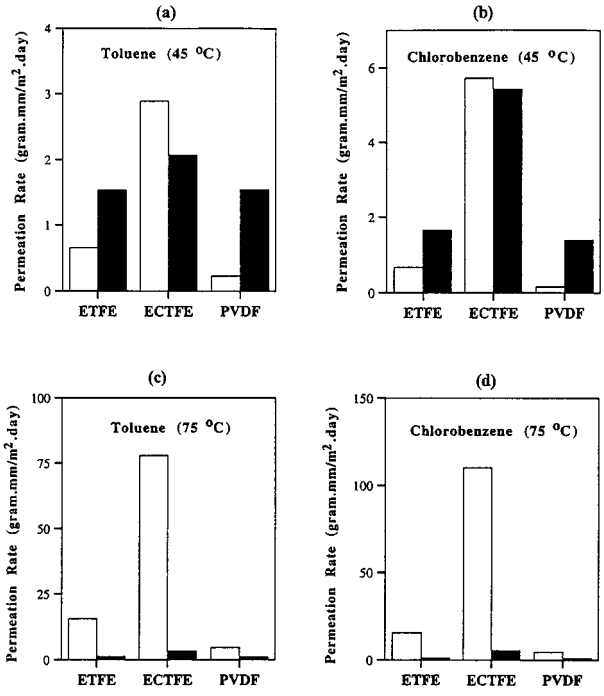

Figure 7 The permeation rates of fluoropolymers with different thicknesses at 45° and 75°C. The units of permeation rate (PC) are (g · mm/m² · day) (□: 0.254 mm, ■: 2.286 mm).

Table V The Permeation Rate of Aromatic Liquids Through Fluoropolymers

Polymer	Temperature (°C)	Permeation Rate: Benzene ($g/m^2/day$)	Permeation Rate: Toluene ($g/m^2/day$)	Permeation Rate: Chlorobenzene ($g/m^2/day$)
ETFE	25.0	0.4794	0.2693	0.3150
	45.0	5.1767	2.5662	2.6293
	75.0	109.8720	61.3581	60.9391
ECTFE	25.0	1.1908	0.7897	1.4061
	45.0	22.3765	11.3682	22.5039
	75.0	693.8069	307.0620	433.7100
PVDF	25.0	0.1153	0.0530	0.0468
	45.0	2.0536	0.9013	0.6268
	75.0	35.1882	18.1996	17.6400

molar volume, polarity, and solubility parameters of penetrating solvents. This section examines the dependence of those transport properties on the preceding thermodynamic properties. The object is to discern whether consistent relationships exist for the various penetrant and polymer combinations.

It is known that PFA resin is nonpolar and highly resistant to chemical attack. As expected, PFA exhibited systematic (but rough) dependence of transport properties only on a geometric factor, i.e., molar volume, as shown in Figure 10(a). Conversely, it showed nonlinear or random dependence on electronic factors such as polarity or solubility parameters, as shown in Figures 10(b) through 10(d).

ETFE exhibited a similar but noisier dependence of permeation rate on molar volume, while other variables such as electronic factors and solubility parameters seemed to have nonlinear or random effects, as shown in Figures 11(a) through 11(d). Generally, the permeation rate showed irregular dependence on penetrant properties.

In contrast, ECTFE exhibited clearer dependence on electronic factors such as polarity (P) and the H-bonding solubility parameter (δ_h), as shown in Figures 12(a) through 12(d). Moderate values of polarity (P) and the H-bonding parameter (δ_h) maximize the permeation rate.

Figures 13(a) through 13(d) show that PVDF exhibited distinct dependence of permeation rate (PR) only on δ_h. Compared with ECTFE, the δ_h

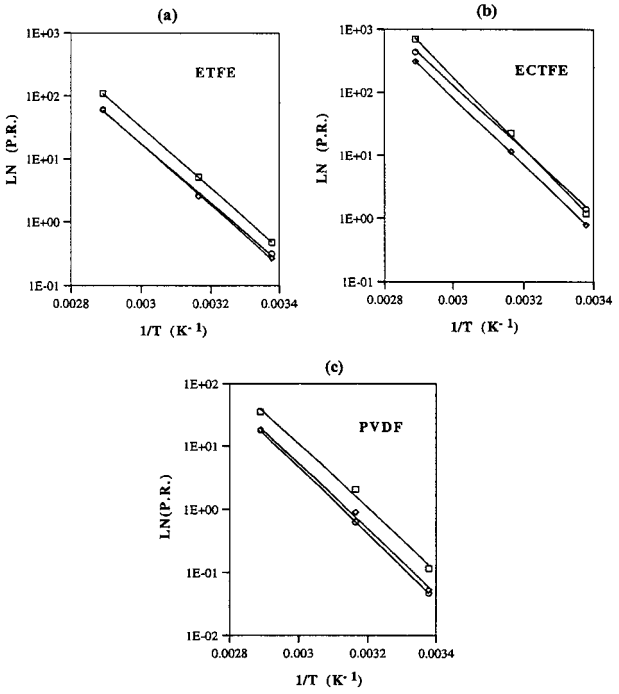

Figure 8 Arrhenius plots of permeation rates of aromatic solvents in fluoropolymers (□: Benzene, ◇: Toluene, ○: Chlorobenzene).

Table VI Activation Energies From Arrhenius Plots [Ln Permeation Rate ($g/m^2/day$) vs. Temperature^{-1} (K^{-1})]

Polymer	Permeation Activation Energy (kcal/mol): Benzene	Toluene	Chlorobenzene
ETFE	465.5	260.1	258.1
ECTFE	2,950	1,304	1,839
PVDF	149.1	77.2	74.9

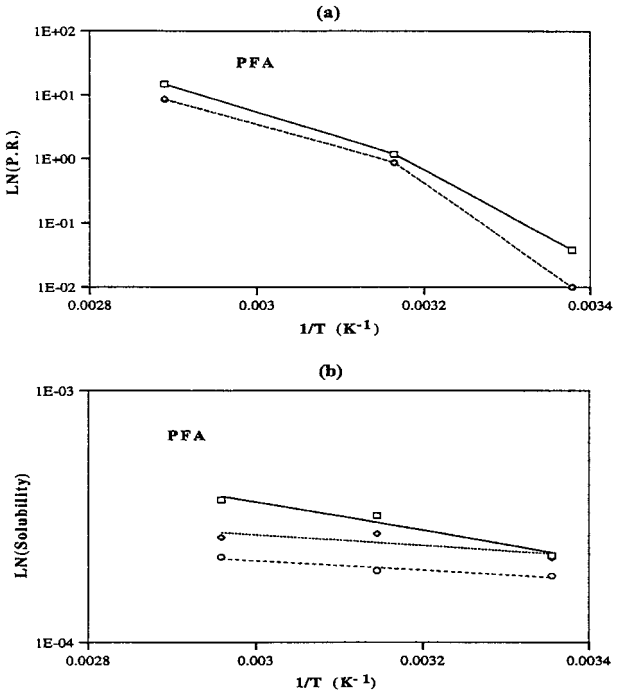

Figure 9 Temperature and penetrant effects on permeation rate and solubility (mol/cm^3) for PFA (□: Benzene, ◇: Toluene, ○: Chlorobenzene).

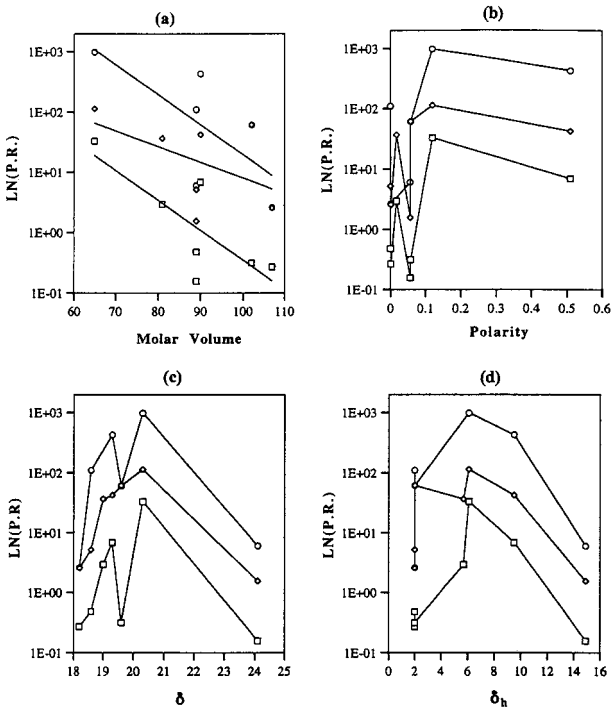

Figure 11 Dependence of permeation rate on thermodynamic properties of penetrants for ETFE polymers (□: 25°C, ◇: 45°C, ○: 75°C).

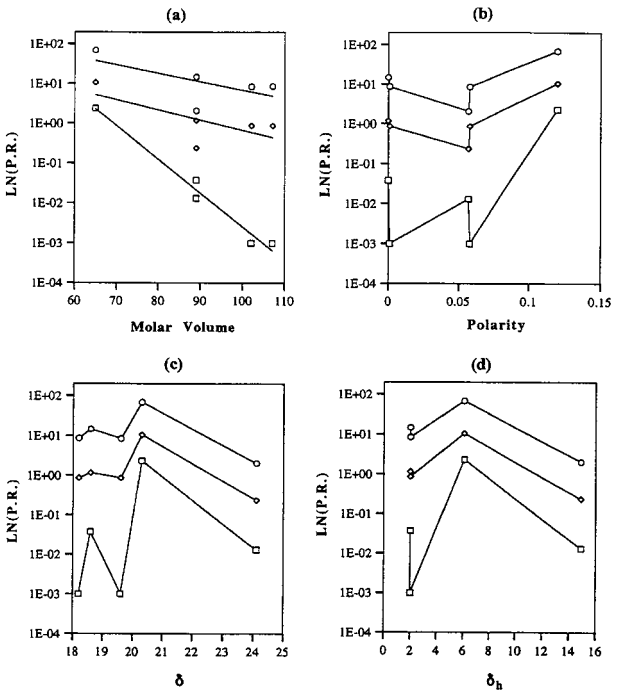

Figure 10 Dependence of permeation rate on thermodynamic properties of penetrants for PFA polymers (□: 25°C, ◇: 45°C, ○: 75°C).

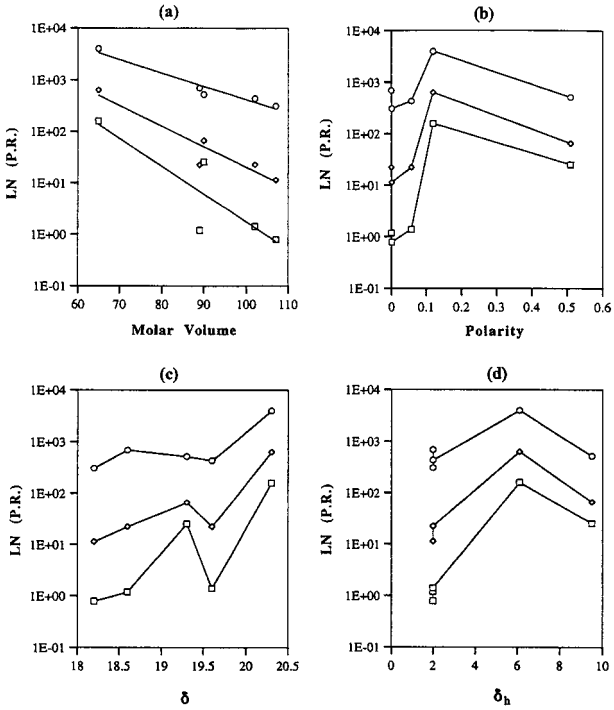

Figure 12 Dependence of permeation rate on thermodynamic properties of penetrants for ECTFE polymers (□: 25°C, ◇: 45°C, ○: 75°C).

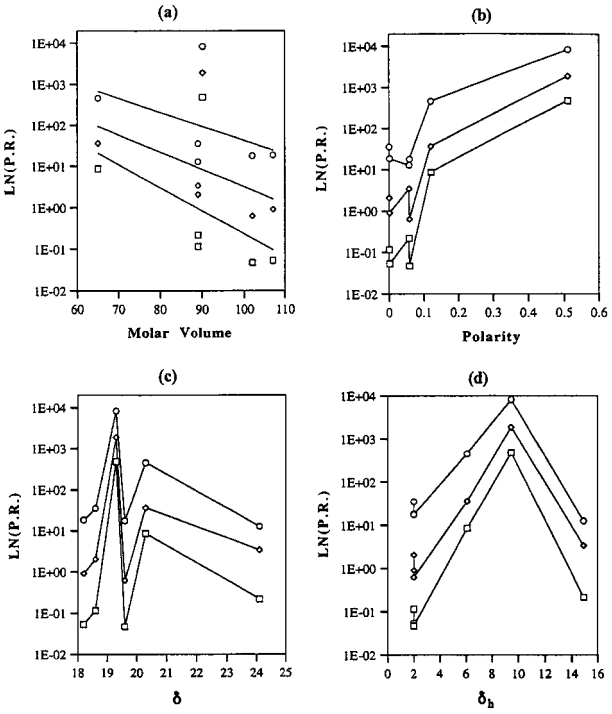

Figure 13 Dependence of permeation rate on thermodynamic properties of penetrants for PVDF polymers (□: 25°C, ◇: 45°C, ○: 75°C).

value of PVDF, at which the maximum permeation rate occurs, shifted from ~ 6 to ~ 10. Furthermore, the permeation rate of PVDF depended more strongly on δ_h than ECTFE. Finally, PVDF was nearly as sensitive to polarity as ECTFE. Both exhibited large increases in permeation rate for polar versus nonpolar penetrants, though ECTFE is less sensitive at high polarity than is PVDF.

CONCLUSIONS

Exposure of fluoropolymer films of different thicknesses to various solvents at several temperatures exhibited a broad range of trends that correspond to their chemical, physical, and processing properties. From several sets of permeation data, it was confirmed that the intersegmental bonds of PVDF are more protonic, and those of ECTFE are more like dipole–dipole interactions. In contrast, ETFE is less polar than ECTFE and less protonic than PVDF. The increase of polar intersegmental attraction produced a high cohesive energy density and resulted in good mechanical and barrier properties. Unfortunately, from the standpoint of barrier characteristics, non-Fickian diffusion was induced by the relaxation-controlled disruption of relatively weak intersegmental bonds due to solvent plasticization, resulting in increased permeability of partially fluorinated polymers as exposure time increased.

Using the same analogy for the relaxation mechanism developed elsewhere for non-Fickian sorption,[17] a kinetic model was devised to explain the observed transient permeation behavior of ECTFE-penetrant systems at 25°C. This model also explained anomalous transient permeation behavior. For example, the permeability ratio for different permeants was within an order magnitude of the corresponding diffusivity ratio. The fitted values, θ and k_{f0}, provided a consistent explanation of experimental observations. That is, the lower θ and k_{f0} values obtained for permeation from the tough, shiny side to the dull, soft side were consistent with the slower transient sorption rates observed and reported elsewhere,[17] probably due to the slower relaxation of the shiny side compared with the dull side.

The generic transport characteristic, the permeation rate, correlates well with physical properties such as molar volume, polarity, and the H-bonding solubility parameter of the penetrants. The relatively inert PFA shows only clear dependence of transport properties on the molecular size of the penetrants. Similarly inert, but structurally modified ETFE, shows similar dependence on molecular size and exhibits nearly random dependence on all the other physical factors. ECTFE, on the other hand, exhibits relatively clear dependence of the permeation rate on molecular size, polarity, and on the H-bonding parameter. Likewise, PVDF exhibits distinct dependence of the permeation rate on the H-bonding parameter. The obtained trends may make it possible to extrapolate or interpolate permeability for other penetrants. In fact, these observations may enable development of a coherent structure–property relationship for transport of diverse fluids in fluoropolymers.

The authors are grateful to Ohio State University for providing facilities for this research. Financial support provided for part of this study and contribution of the polymer samples used in this study by E. I. duPont de Nemours & Co. is gratefully acknowledged. In addition, many helpful suggestions were made by Dr. Sina Ebnesajjad.

REFERENCES

1. C. E. Rogers, in *Polymer Permeability,* J. Comyn, Ed., Elsevier Applied Science Publishers Ltd., London, 1985, Chap. 2.

2. X. Q. Nguyen, M. Sipek, and Q. T. Nguyen, *Polymer,* **33,** 3699 (1992).
3. J. Crank and G. S. Park, *Diffusion in Polymers,* Academic Press (1968).
4. J. H. Hildebrand, *J. Am. Chem. Soc.,* **41,** 1067 (1919).
5. C. M. Hansen, *Ind. Eng. Chem. Pro. Develop.,* **8,** 2 (1969).
6. T. Graham, *Phil. Mag.,* **32,** 401 (1866).
7. R. M. Barrer, *J. Am. Chem. Soc.,* **56,** 278 (1934).
8. R. M. Barrer, *Trans. Faraday Soc.,* **35,** 628–644 (1939).
9. F. Doghieri, G. Camera-Roda, and G. C. Sarti, *AIChE J.,* **39,** 1847 (1993).
10. C. Cattaneo, *Atti Sem. Mat.,* **3,** 83 (1948).
11. G. Camera-Roda and G. C. Sarti, *Trans. Theory Stat. Physics,* **15,** 1023 (1986).
12. G. Camera-Roda and G. C. Sarti, *AIChE J.,* **36,** 851 (1990).
13. G. Camera-Roda, F. Doghieri, T. A. Ruggeri, and G. C. Sarti, in *Nonlinear Waves and Dissipative Effects,* D. Fusco and A. Jeffrey, Eds., Longman Scientific & Technical Hallow, UK, 1991, p. 182.
14. M. N. Ozisik and B. Vick, *Int. J. Heat Mass Transfer,* **27,** 1845 (1984).
15. J. Crank, *The Mathematics of Diffusion,* 2nd ed., Oxford University Press, Oxford (1975).
16. A. R. Berens and H. B. Hopfenberg, *Polym.,* **19,** 489 (1978).
17. S. W. Lee and K. S. Knaebel, "Effects of Mechanical and Chemical Properties on Transport in Fluoropolymers. I. Transient Sorption," to appear.
18. C. E. Rogers, V. Stannett, and M. Szwarc, *J. Polym. Sci.,* **45,** 61 (1960).
19. H. T. Kim and R. S. Brodkey, *AIChE J.,* **14,** 61 (1968).
20. J. I. Gordon, *J. Paint Technol.,* **38,** (492), 43 (1966).
21. J. S. Vrentas, C. M. Jarzebski, and J. L. Duda, *AIChE J.,* **21,** 895 (1975).
22. Clark, E. S., Paper Given at Symposium on Helices in Macromolecular Systems, Polytechnic Institute of Brooklyn, Brooklyn, NY, May 16, 1959.